JOURNAL OF MATERIALS SCIENCE 14 (1979) 1457–1464

Critical currents of *in situ* formed multifilamentary Cu–Nb_3Sn composites

J. BEVK, JAMES P. HARBISON
Division of Applied Sciences, Harvard University, Cambridge, Massachusetts 02138, USA

Critical current densities of *in situ* formed Cu–Nb_3Sn composites with discontinuous filaments were measured as a function of superconducting volume fraction, matrix resistivity, area reduction ratio, and applied magnetic field. In agreement with recent modelling by Tinkham and co-workers, the effective superconducting volume fraction in a given composite was found to be field-dependent, necessitating the distinction between microstructural and electrical percolation. In composites with a low filament volume fraction, proximity effect coupling, controlled by matrix resistivity, was found to be the dominant factor determining both the composite remnant resistivity and the critical current density. For sufficiently high filament volume fractions and area reduction ratios, the remnant resistivities fall below the level of detection, as predicted by theory, and critical current densities become comparable to those of continuous filament composites. SEM, TEM, and STEM analysis reveal a dense distribution of submicron, ribbon-like Nb_3Sn filaments in relatively pure Cu matrix. The microstructure of the filaments is equi-axed with an average grain size of ~ 400 Å, ensuring effective flux pinning.

1. Introduction

A number of recent investigations on *in situ* formed Cu–Nb–Sn superconducting composites [1–5] have demonstrated that these conductors are interesting not only as model systems for the study of transport properties in multiphase materials but also as practical conductors. Besides high critical temperature, T_c, and critical current density, J_c, we recently reported on two other important aspects of these composites related to their stability: high resistance to plastic deformation and extremely low matrix resistivity [2].

The mechanisms which lead to a vanishingly small resistance in these conductors with *discontinuous* filaments are not yet fully understood. Tsuei [6] suggested that proximity effect might play an important role in interfilament coupling; on the other hand, Davidson *et al.* [7] demonstrated, by means of a simple geometrical model, that for sufficiently large reductions in cross-sectional area, the composite resistivity would be undetectable even if the matrix remains completely normal. Some of the experimental features they observed suggested a percolation threshold, attributed indirectly to the proximity effect. Other explanations include the existence of superconducting bridges due to the presence of small superconducting precipitates between the filaments [8] and a physically interconnected filament network above the percolation threshold [7, 9].

In this paper we report results on *in situ* formed composites containing superconducting volume fractions both above and below the predicted [10, 11] percolation threshold (15 ± 2 vol%). This allows us to look both at the regime well below the percolation threshold where measured remnant resistivities are of interest and at the high filament volume fraction regime where high critical current densities, comparable to those found in the best continuous filament composites, are observed.

2. Experimental details

The experimental procedure was essentially the same as that described in greater detail elsewhere [2, 12]. Samples were prepared metallurgically by

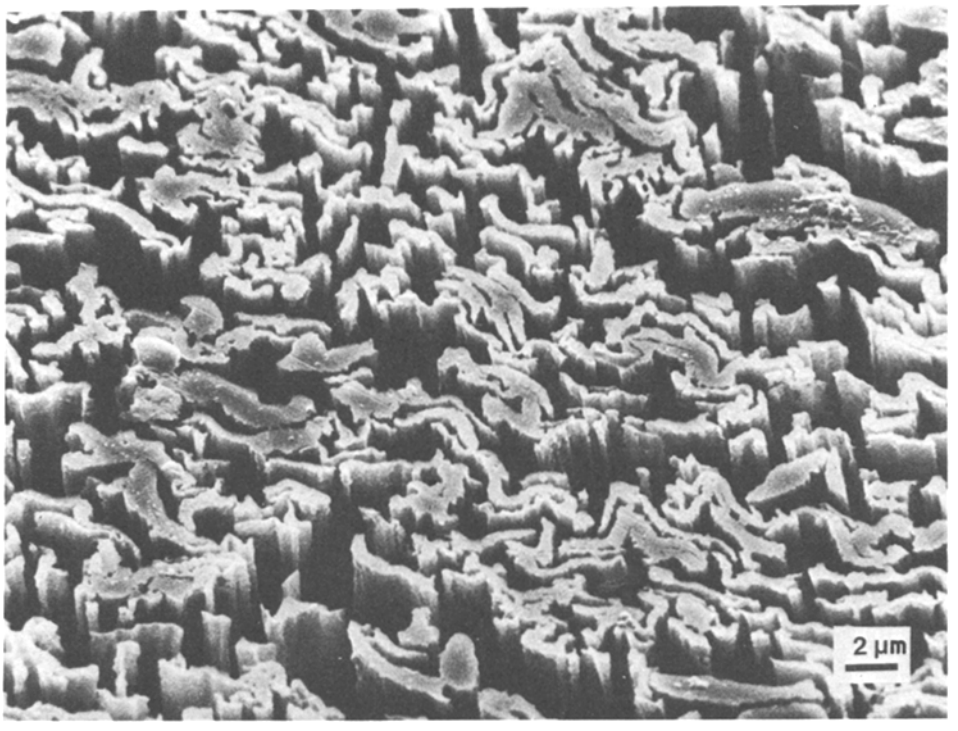

Figure 1 Scanning electron micrograph of a transverse cross-section of a 0.53 mm diameter $Cu_{88}Nb_{10}Sn_2$ composite wire, etched lightly to reveal the ribbon-like filaments.

melting together the three constituent elements using an r.f. levitation melting technique which ensured adequate mixing. The final melting of each of the 10 to 12 g charges was performed in a vertical water-cooled container, again using r.f. heating, which provided a controlled cooling rate on the order of 500° C sec^{-1}. The ingots, consisting of an array of niobium precipitates in a surrounding copper–tin matrix, were then swaged and drawn down to cross-sectional area reductions varying from 40 to 160. Finally, in order to form the Nb_3Sn layer, the wires were heat-treated at either 650 or 700° C for times ranging from 12 to 48 h.

Optical microscopy was used on unreduced ingots to determine both the uniformity and size distribution of the precipitates. The final wires were polished and lightly etched to remove a layer of matrix material and then examined in a scanning electron microscope. Samples from both the annealed and unannealed wires were mechanically polished to a thickness of 50 μm and then thinned in an ion micro-miller for observation in a transmission electron microscope.

The current–voltage characteristics of each of the annealed wires were determined as a function of applied transverse magnetic field using a 150 kG solenoid. Contact heating precluded measurements in the lowest fields due to the excessively high currents. The overall critical current density, J_c, was defined as the current at which the voltage drop across 8 mm of the wire exceeded 1 μV (the lowest voltage detectable above the magnet-induced voltage noise), normalized to the entire cross-section of the wire. In wires with a low volume fraction of superconductor where remnant resistance was clearly observed even at zero current, the value of critical current used for comparison was the point at which the I–V curve departed by 1 μV from the linear resistive baseline.

3. Results and discussion

Fig. 1 shows a scanning electron micrograph of a Cu–Nb–Sn composite after mechanical reduction to a wire 0.53 mm diameter. The etched surface reveals a uniform, dense distribution of Nb–Sn filaments with a ribbon-like shape, indicative of a plane-strain deformation mode during mechanical reduction [12]. The filaments, as seen in Fig. 1, have a smaller effective diameter than in the case of axially symmetric flow and the diffusion distances are correspondingly shorter. This allows for short annealing times at relatively low temperatures and, in turn, small grain size. Since the flux-pinning force in most A-15 compounds, including

TABLE I Summary of critical current and resistivity measurements

Specimen number	Composition (at. %)	Diameter (mm)	Reduction ratio* R	Annealing temperature (°C)	Annealing time (h)	Resistivity ratio†	Low temperature resistivity‡ ($\mu\Omega$ cm)	Average tin conc. in matrix§ (at. %)	Overall J_c (4.2 K) (A cm^{-2}) at				
									40 kG	80 kG	100 kG	120 kG	150 kG
1	$Cu_{84}Nb_{12.5}Sn_{3.5}$	0.51	160	650	12	4.23	0.87	0.25	–	–	$> 1.4 \times 10^4$	$> 1.2 \times 10^4$	3.1×10^3
2		0.51	160	650	24	9.40	0.27	0.078	–	3.4×10^4	1.8×10^4	8.4×10^3	1.4×10^3
3		0.51	160	650	48	12.14	0:21	0.061	–	4.0×10^4	2.3×10^4	1.2×10^4	2.4×10^3
4	$Cu_{84}Nb_{12.5}Sn_{3.5}$	0.76	70	650	12	2.49	1.8	0.52	–	$> 2.8 \times 10^4$	2.2×10^4	1.2×10^4	2.6×10^3
5		0.76	70	650	24	4.15	0.78	0.23	–	$> 2.8 \times 10^4$	2.5×10^4	1.3×10^4	3.1×10^3
6		0.76	70	650	48	3.75	0.88	0.25	–	$> 2.8 \times 10^4$	2.0×10^4	1.1×10^4	2.1×10^3
7	$Cu_{84}Nb_{12.5}Sn_{3.5}$	1.02	40	650	12	1.97	2.8	0.81	$> 1.5 \times 10^4$	$> 1.2 \times 10^4$	9.7×10^3	6.6×10^3	1.7×10^3
8		1.02	40	650	24	2.15	2.2	0.64	–	–	–	–	2.7×10^3
9		1.02	40	650	48	2.70	1.5	0.44	–	$> 1.4 \times 10^4$	$> 1.3 \times 10^4$	7.4×10^3	2.0×10^3
10	$Cu_{87}Nb_{10}Sn_3$	0.61	110	650	96	7.90	0.50	0.15	2.8×10^4	1.2×10^4	8.0×10^3	3.3×10^3	9.4×10^2
11	$Cu_{87.5}Nb_{10}Sn_{2.5}$	0.58	120	650	96	3.99	0.94	0.28	1.9×10^4	5.5×10^3	–	1.7×10^3	2.9×10^2
12	$Cu_{87.5}Nb_{10}Sn_{2.5}$	0.58	120	700	48	4.11	0.84	0.25	$> 1.9 \times 10^4$	9.5×10^3	5.6×10^3	2.6×10^3	4.4×10^2
13	$Cu_{88}Nb_{10}Sn_2$	0.53	140	650	48	19.5	0.14	0.042	2.3×10^4	8.0×10^3	3.8×10^3	1.5×10^3	2.9×10^2
14	$Cu_{88}Nb_{10}Sn_2$	0.53	140	700	12	6.47	0.53	0.16	$> 1.8 \times 10^4$	8.4×10^3	4.5×10^3	2.0×10^3	2.9×10^2
15	$Cu_{92}Nb_5Sn_3$	0.51	160	650	12	1.60	4.1	1.33	2.3×10^3	7.2×10^2	4.0×10^2	1.7×10^2	3.0×10^1
16		0.51	160	650	24	2.17	2.7	0.88	6.8×10^3	2.7×10^3	1.4×10^3	5.9×10^2	–
17		0.51	160	650	48	2.87	1.7	0.55	1.1×10^4	4.5×10^3	2.6×10^3	1.2×10^3	2.5×10^2
18	$Cu_{92}Nb_5Sn_3$	0.76	70	650	12	1.38	6.4	2.09	7.2×10^1	3.5×10^1	1.9×10^1	1.5×10^1	6.9×10^0
19		0.76	70	650	24	1.38	6.2	2.03	–	–	–	–	–
20		0.76	70	650	48	1.35	5.8	1.90	–	–	–	3.0×10^1	7.9×10^0
21	$Cu_{92}Nb_5Sn_3$	1.02	40	650	12	1.28	7.3	2.39	9.6×10^1	4.4×10^1	3.8×10^1	2.5×10^1	7.4×10^0
22		1.02	40	650	24	1.31	7.2	2.37	1.0×10^2	4.3×10^1	5.2×10^1	3.3×10^1	–
23		1.02	40	650	48	1.37	6.7	2.18	5.7×10^1	5.1×10^1	3.2×10^1	2.3×10^1	6.0×10^0

* Ratio of initial ingot cross-sectional area to final wire cross-sectional area.

† Ratio of resistivity at room temperature to that just above T_c.

‡ At a temperature just above T_c.

§ After annealing.

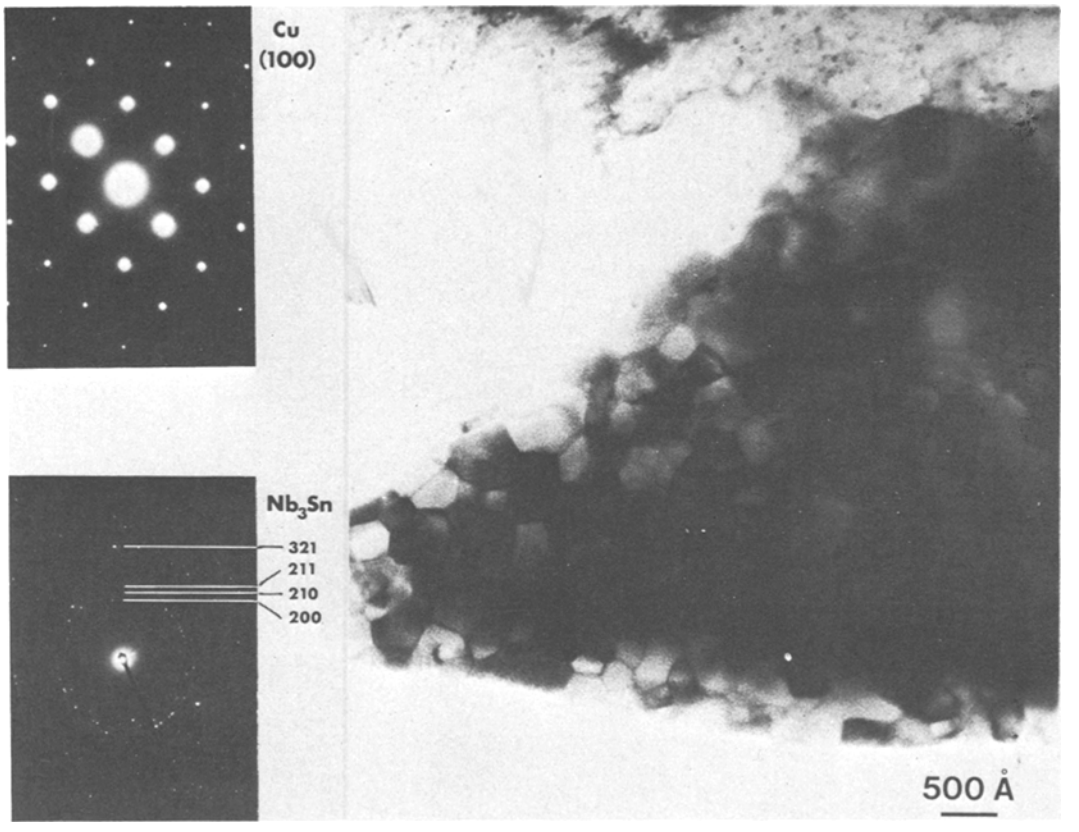

Figure 2 Transmission electron micrograph of an annealed $Cu_{84}Nb_{12.5}Sn_{3.5}$ composite showing the fine, equi-axed grain structure in the filamentary material. The diffraction patterns are from the copper matrix and the Nb_3Sn filament.

Nb_3Sn, where the primary source of pinning are grain boundaries, is inversely proportional to the grain size, high critical currents should be expected in such materials with extremely fine microstructure.

Fig. 2 shows a transmission electron micrograph of a Cu–Nb–Sn composite, 0.51 mm diameter, after annealing at 650° C for 48 h. The Nb_3Sn grains appear to be equi-axed with an average grain size of ~ 400 Å, considerably smaller than in conventional composite tapes or wires. The broad beam diffraction pattern from the Nb_3Sn filament is compatible with the A-15 structure; it shows no significant preferred orientation in contrast to the case prior to annealing in which the niobium filaments possess a well-defined ⟨1 1 0⟩ orientation due to texture formation. The diffraction pattern and the contrast from the matrix in Fig. 2 are typical for recrystallized material. The X-ray analysis and element mapping obtained by scanning-transmission electron microscope (Fig. 3) show that in the annealed specimens, essentially all the tin has diffused from the matrix into the filaments to form Nb_3Sn, the signal from tin being at the background noise level. This observation is consistent with the measurements of residual electrical resistivity which will be discussed later.

The critical current density results are summarized in Table I. For comparison, the highest J_c values obtained in our previous study of $Cu_{88}Nb_{10}Sn_2$ and $Cu_{87.5}Nb_{10}Sn_{2.5}$ composites are also included (specimens 11–14).

It is clear that J_c increases significantly by increasing both the volume fraction of niobium and the initial tin content in the matrix. By keeping the niobium content constant at 10 at.% and increasing the tin concentration by only ½% (from 2.5 to 3 at.%), J_c increases by almost a factor of two at high fields, with a smaller yet still significant increase at lower fields. This is at least partially due to the fact that the superconducting filaments in the $Cu_{87}Nb_{10}Sn_3$ sample are much closer to the ideal 3:1 niobium-to-tin ratio.

Increasing the niobium content has an even

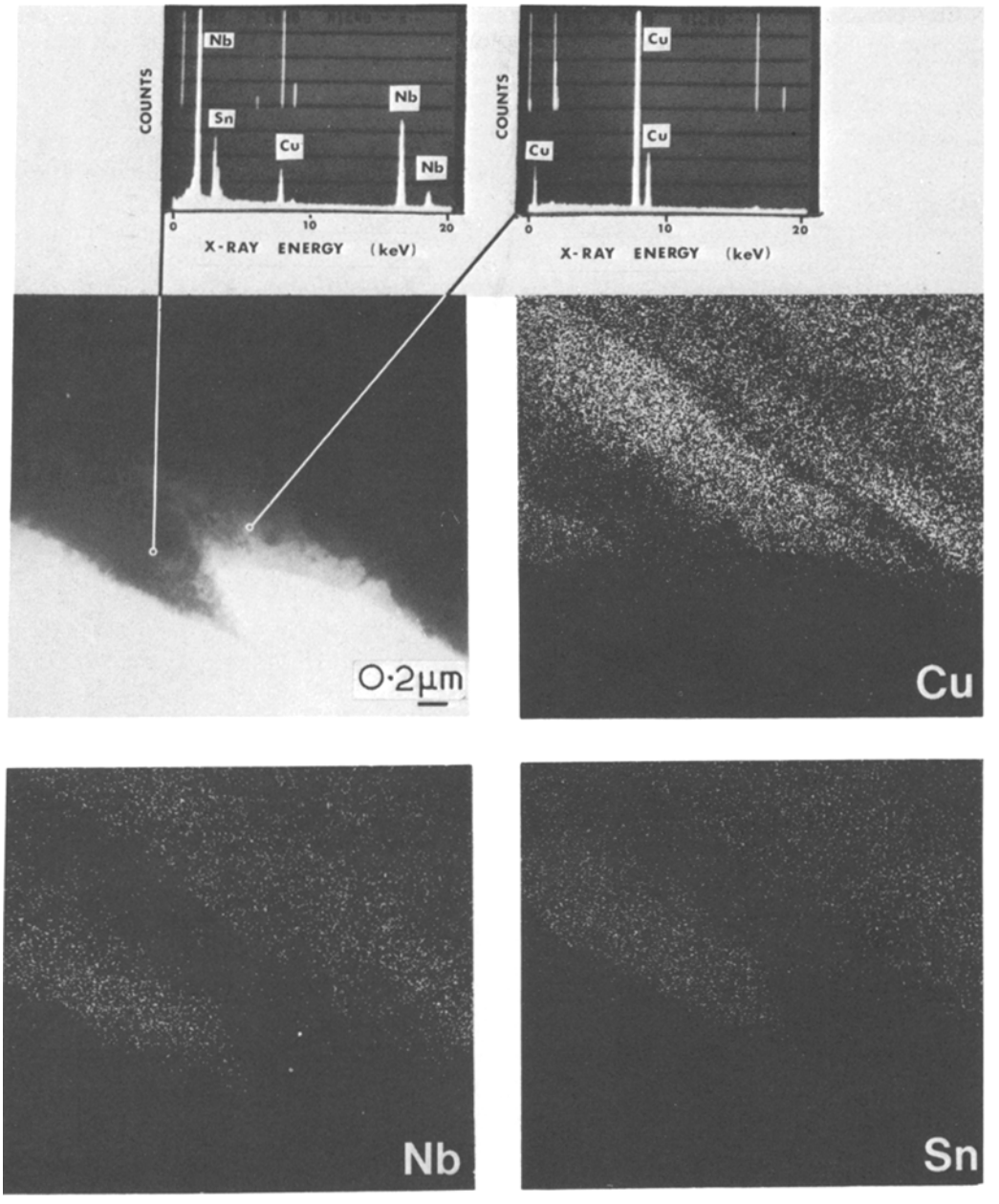

Figure 3 Scanning transmission electron micrograph, (a) of the area shown in Fig. 2, and the corresponding elemental maps for (b) copper, (c) niobium and (d) tin. At the top of the figure are X-ray energy dispersive analysis spectra from the centre of the filament (left) and matrix (right).

more pronounced effect on the current carrying capacity of these wires; the highest J_c values for the $Cu_{84}Nb_{12.5}Sn_{3.5}$ samples are a factor of five above the best 10 at.% Nb values reported previously [2]. In fact, the overall critical current density of the best *in situ* composites measured here is comparable to that of conventional continuous-filament Cu–Nb_3Sn conductors and can possibly be further improved. More important, both the matrix conductivity and the mechanical strength are significantly higher than the values reported in the literature for conventional composites. In the case of the better $Cu_{84}Nb_{12.5}Sn_{3.5}$ samples, the low temperature matrix resistivity values, listed in Table I, are $\sim 0.2\,\mu\Omega$ cm, appreciably lower than reported values for *in situ* composites formed by external diffusion [5], and about a factor of 20 lower than in conventional

Cu–Nb_3Sn composites. This difference represents a key advantage in terms of the overall stability of the composite as supplied by the surrounding matrix. In addition, because of the strengthening mechanisms which come into play when the filament diameter and interfilament spacing become sufficiently small, the mechanical properties of these *in situ* composites are greatly improved over their conventional counterparts [2, 12].

Before turning to the results for the $Cu_{92}Nb_5Sn_3$ composition, which was chosen to study the characteristics of an *in situ* formed composite below the superconducting percolation threshold, it is important at this point to make the distinction between microstructural and electrical percolation. Microstructural percolation requires a continuous path of Nb–Nb_3Sn material from one end of the conductor to the other, whereas electrical percolation merely requires a continuous path of "superconducting" material, where some of the surrounding copper–tin matrix falls into this "superconducting" category because of the proxmity effect. Since for the high aspect ratio filaments considered in this study this extra sheath of proximity-effect-induced superconducting Cu–Sn around each filament can be comparable in volume to the actual filament material, one would expect the threshold for electrical percolation to occur at a considerably lower filament volume fraction than the threshold for microstructural percolation. The degree of the discrepancy between the two depends primarily on the matrix coherence length which is a function of the mean free path in the matrix material. A study of these effects in Cu–Nb *in situ* formed composites is covered by Lobb *et al.* elsewhere [13].

Only slightly above the threshold, percolation theory predicts not just one but many continuous paths through the Nb–Sn material. One therefore expects to find a sponge-like, interconnected network of filamentary material throughout the composite. However, when the composites considered in the present study are etched until the matrix material is completely dissolved, the individual filaments fan out away from one another in a brush-like fashion [2], indicating the lack of such cross-linkage or sponge-like interconnections. This behaviour was observed even in the composites with the highest volume fraction of filaments, thus placing the microstructural percolation threshold above 18.2 vol % Nb (12.5 at.%).

It should be noted that the theoretically predicted percolation threshold of 15 ± 2 vol % is based on an idealized random system. For a real system, such as Cu–Nb or Cu–Nb–Sn, this value can be much higher because during the formation of the dendritic structure, contact between adjacent precipitates is discouraged. However, precipitation kinetics can be altered drastically in the presence of small amounts of impurities, such as carbon or oxygen. Verhoeven *et al.* [5] investigated this effect in detail by melting Cu–Nb alloys in different types of crucibles followed by chill-casting. They observed a variety of microstructures ranging from a "flower-like" configuration of Nb particles when using graphite crucibles, as previously reported by Roberge and co-workers [9, 14] to a dendrite morphology, similar to ours, when using thoria crucibles. The difference in the observed microstructures was correlated with the impurity content and supports our earlier contention [15] that the microstructural percolation threshold in Cu–Nb is not a well-defined value but depends sensitively on a number of experimental parameters such as quenching rate, impurity concentration, etc. Such considerations are clearly important when evaluating properties such as a.c. losses and stability.

As discussed above, the electrical percolation threshold is a strong function of the degree of proximity effect coupling and hence dependent upon the electron mean free path in the matrix. Davidson and co-workers [7, 16, 17] were able to detect, using a very sensitive SQUID voltmeter, a remnant resistance plateau in the resistance versus temperature curves for a $Cu_{93.5}Nb_5Sn_{1.5}$ composite, but saw no such plateau in a $Cu_{88.5}Nb_{10}Sn_{1.5}$ composite, presumably indicating electrical percolation. In order to look at the high-current behaviour of composites clearly below this electrical percolation threshold, we prepared a new series of samples with the composition $Cu_{92}Nb_5Sn_3$. The excessive amount of tin was chosen to ensure a "dirty" matrix after annealing, thus further reducing proximity effect coupling.

The result is a qualitative change in the shape of the I–V curves of the wires of this composition as compared to the higher filament volume fraction samples. Instead of remaining flat up to very high current densities, the curves for the wires with only 5 at.% Nb (7.6 vol %) display a positive slope already at the origin, indicative of a remnant resistivity, ρ_{REM}.

The values of the zero field remnant resistivity

TABLE II Zero-field remnant resistivities

Diameter (mm)	Annealing time at 650° C (h)	Reduction ratio R (A/A_0)	Normal state composite resistivity ρ_0 (10^{-6} Ω cm)	$\rho_{REM}^{(H=0)}$ (Ω cm)	DBT theory* $\frac{\rho_0}{f_s R^3}$
0.51	12	160	4.1	$< 1.2 \times 10^{-11}$	1.3×10^{-11}
0.51	24	160	2.7	$< 1.7 \times 10^{-11}$	8.7×10^{-12}
0.51	48	160	1.7	$< 2 \times 10^{-11}$	5.5×10^{-12}
0.76	12	70	6.4	2.5×10^{-8}	2.5×10^{-10}
0.76	24	70	6.2	$< 8 \times 10^{-8}$	2.4×10^{-10}
0.76	48	70	5.8	$< 1.1 \times 10^{-8}$	2.2×10^{-10}
1.02	12	40	7.3	7.7×10^{-9}	1.5×10^{-9}
1.02	24	40	7.2	9.4×10^{-8}	1.5×10^{-9}
1.02	48	40	6.7	$3\,3 \times 10^{-8}$	1.4×10^{-9}

* f_s, the superconducting volume fraction, is assumed to be the original volume fraction of Nb, i.e. 0.076.

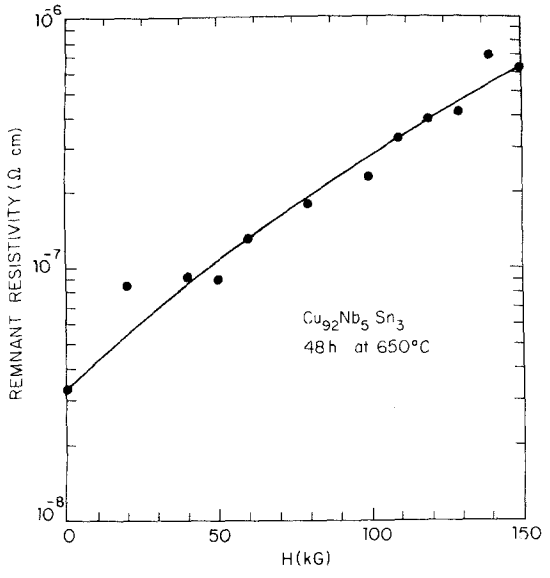

Figure 4 Remnant resistivity below the superconductive transition as a function of applied transverse magnetic field in a 1 mm diameter composite containing only 5 at.% niobium.

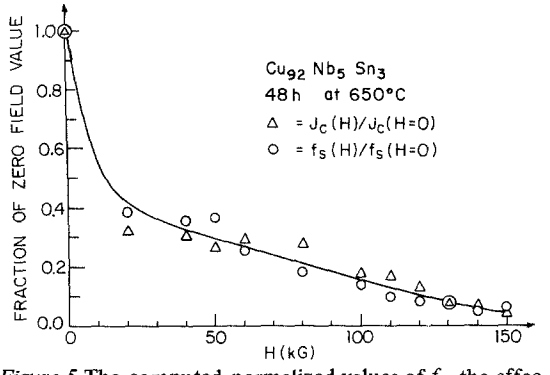

Figure 5 The computed normalized values of f_s, the effective superconducting volume fraction (open circles), as a function of field for the same specimen as that in Fig. 4, plotted together with the corresponding normalized J_c values (open triangles).

for each of the 5 at.% Nb specimens tested are listed in Table II. These values are compared with the predictions of the theory of Davidson *et al.* [7] in which these discontinuous-filament composites are modelled by a regular three-dimensional array of finite-length superconducting rods embedded in a normal matrix. Such a model is clearly an oversimplification and is intended more to predict qualitatively the dependence of ρ_{REM} on composite area reduction, R, than to give its exact value. Still, as is evident in Table II, the absolute values for the remnant resistivity predicted by the theory are in general order of magnitude agreement with the experimental values we measured. The agreement is even better if the correction is made for the experimental observation that, during the early stages of reduction, the niobium precipitates deform at a lower rate than the surrounding matrix material. Our samples do not span a wide enough range of reduction, because of the rapid work-hardening of the copper–tin matrix, to test the $1/R^3$ dependence.

The determination of ρ_{REM} from the I–V curves allows us to measure this quantity also as a function of applied magnetic field. Fig. 4 shows that, with increasing field, ρ_{REM} increases appreciably, as one would expect. The applied field both weakens the proximity effect coupling and drives normal the "weaker", off-stoichiometric Nb_3Sn, thus causing the transport current to traverse more normal material. Within the context of the Davidson–Beasley–Tinkham theory mentioned above, which predicts that

$$\rho_{REM} = \frac{\rho_0}{f_s R^3},$$

one could think of this effect simply as the result of a decreasing superconducting volume fraction, f_s, due to the effects mentioned above. At low temperatures, the magnetoresistance effect in pure metals in high fields can be significant (a factor of 4 for Cu at 150 kG [19]). However, in the present composites, where the electron mean free path is much shorter due to the dirty matrix, the effect is only on the order of a few per cent, and hence ρ_0, the normal-state composite resistivity, can effectively be considered a constant. Under these simple assumptions, we can then generate a curve of the effective f_s as a function of field, with the individual data points shown as open circles in Fig. 5. As indicated by the open triangles in the same figure, the normalized critical current density, defined earlier as the point of departure from the initial remnant resistivity baseline, follows the same functional dependence as the computed f_s. Upon further reduction the normal state resistivity of wires of this composition gradually decreases (see Table II) while the remnant resistivity falls precipitously below the level of detection. The accompanying rapid increase in J_c by about two orders of magnitude strongly suggests that the current carrying capacity of these composites depends more on proximity effect coupling, dictated by the properties of the matrix, than on the characteristics of the superconducting filamentary material itself.

In conclusion, an analysis of the $I-V$ curves of the *in situ* composites with a low volume fraction of superconducting filaments and low area-reduction ratios clearly indicates that the proximity effect plays an important role in the transport behaviour of these materials. In composites with higher filament volume fraction reduced to smaller size, the remnant resistivity drops to undetectable values, and the overall critical current densities compare favourably with those of conventional composites. In addition, excellent mechanical properties and high matrix conductivity should provide high overall stability – an important requirement for practical applications.

Acknowledgements

The authors would like to thank M. Tinkham, W. J. Skocpol and C. Lobb for their helpful discussions regarding the percolation aspects of this work. They gratefully acknowledge JEOL for making available a 100-CX electron microscope, D. F. Harling and T. Yoshioka for their expert help with STEM analysis and E. Seling for his scanning electron microscopy. They extend their thanks to the Francis Bitter National Magnet Laboratory for the use of the high-field magnets and to the National Science Foundation for support of this research through grants DMR-74-22264, DMR-76-01111 and BMS-74-12494. One of the authors (J. P. H.) gratefully acknowledges a postdoctoral Fellowship from the IBM Corporation.

References

1. C. C. TSUEI, M. SUENAGA and W. B. SAMPSON, *Appl. Phys. Letters* **25** (1974) 318.
2. J. P. HARBISON and J. BEVK, *J. Appl. Phys.* **48** (1977) 5180.
3. S. FONER, E. J. McNIFF Jr., B. B. SCHWARTZ and R. ROBERGE, *Appl. Phys. Letters* **31** (1977) 853.
4. R. BORMANN, L. SCHULTZ and H. C. FREYHARDT, *ibid* **32** (1978) 79.
5. J. D. VERHOEVEN, D. K. FINNEMORE, E. D. GIBSON, J. E. OSTENSON and L. F. GOODRICH, *ibid* **33** (1978) 101.
6. C. C. TSUEI, *Science* **180** (1973) 57.
7. A. DAVIDSON, M. R. BEASLEY and M. TINKHAM, *IEEE Trans. Mag.* **MAG-11** (1975) 276.
8. L. SCHULTZ and R. BORMANN, *J. Appl. Phys.* **50** (1979) 418.
9. R. ROBERGE and J. L. FIHEY, *J. Appl. Phys.* **48** (1977) 1327.
10. H. SCHER and R. ZALLEN, *J. Chem. Phys.* **53** (1970) 3759.
11. R. ZALLEN and H. SCHER, *Phys. Rev.* **B4** (1971) 4471.
12. J. BEVK, J. P. HARBISON and J. L. BELL, *J. Appl. Phys.* **49** (1978) 6031.
13. C. J. LOBB, M. TINKHAM and W. J. SKOCPOL, *Solid State Commun.* **27** (1978) 1273.
14. J. L. FIHEY, P. NGUYEN-DUY and R. ROBERGE, *J. Mater. Sci.* **11** (1976) 2307.
15. J. BEVK, J. P. HARBISON and J. L. BELL, TMS-AIME Fall Meeting, Chicago (1977) (unpublished).
16. A. DAVIDSON, Ph.D. thesis, Harvard University (1976).
17. A. DAVIDSON and M. TINKHAM, *Phys. Rev.* **B13** (1976) 3261.
18. J. L. OLSEN and L. RINDERER, *Nature* **173** (1954) 682.

Received 18 September and accepted 1 November 1978.